



This is the accepted manuscript made available via CHORUS. The article has been published as:

Quantum correlations in metals that grow in time and space

T. R. Kirkpatrick and D. Belitz

Phys. Rev. B **93**, 125130 — Published 21 March 2016

DOI: [10.1103/PhysRevB.93.125130](https://doi.org/10.1103/PhysRevB.93.125130)

Quantum Correlations in Metals that Grow in Time and Space

T.R. Kirkpatrick¹ and D. Belitz²

¹*Institute for Physical Science and Technology, University of Maryland, College Park, MD 20742*

²*Department of Physics and Institute for Theoretical Science, University of Oregon, Eugene, OR 97403*

We show that the correlations of electrons with a fixed energy in metals have very anomalous time and space dependences. Due to soft modes that exist in any Fermi liquid, combined with the incomplete screening of the Coulomb interaction at finite frequencies, the correlations in 2-d systems grow as the square of a time scale. In the presence of disorder, the spatial correlations grow as a distance squared. Similar, but in general weaker, effects are present in 3-d systems and in the absence of quenched disorder. We propose ways to experimentally measure these anomalous correlations.

PACS numbers: 05.30.Fk; 71.27.+a

I. INTRODUCTION

Equilibrium time-correlation functions are an essential concept in statistical mechanics.¹ They describe the spontaneous fluctuations of a system in equilibrium, and together with the partition function they provide a complete description of the equilibrium state. Via the fluctuation-dissipation theorem they also describe the linear response of the system to external fields, and they are directly measurable by means of scattering experiments. For instance, the number or charge-density correlation function provides the scattering cross-section for electron, light, or neutron scattering, and the spin-density correlation function the one for magnetic neutron scattering.

An old, and seemingly plausible, assumption is that microscopic correlations decay on time scales much faster than macroscopic observation times; i.e., that there is a separation of time scales. In this paper we study a class of quantum correlation functions for which this is not true, and which actually *grow* as functions of both space and time. Our considerations are exact in the sense that they deal with long-wavelength and low-frequency effects that can be controlled by means of renormalization-group arguments applied to an effective field theory.^{2,3}

We first put the above statements in a historical context. Various concepts that were developed in the early days of statistical mechanics depend on the separation-of-time-scales assumption, for instance, the notion that the BBGKY hierarchy of classical kinetic equations can be truncated,⁴ or the Kadanoff-Baym scheme of deriving and solving quantum kinetic equations and its generalizations.^{5,6} The notion of a separation of time scales is also important in signal processing, where the microscopic time scale associated with the generation of the radiation is typically much faster than the observational time scale.^{7,8} For time-correlation functions it implies that they decay exponentially for large times. Equivalently, their Laplace transform is an analytic function of the complex frequency z at $z = 0$. The discovery of the non-exponential decay known as long-time tails (LTTs),^{9–11} and the related breakdown of a virial expansion for transport coefficients^{12,13} thus came as a consid-

erable surprise,¹⁴ since it showed that the assumption is in general not true. Rather, many time-correlation functions decay only algebraically, i.e., they have no intrinsic time scale. This scale invariance is reminiscent of the behavior of correlation functions at critical points; however, it occurs in entire phases and therefore is referred to as ‘generic scale invariance’.^{15–17} The underlying physical reason is either conservation laws, or Goldstone modes that lead to a slow decay of some long-wavelength fluctuations and, via mode-mode-coupling effects, affect the decay of other degrees of freedom. An example is the shear stress in a classical fluid, which is not conserved, yet its time-correlation function decays algebraically as $1/t^{d/2}$ for long times t in a d -dimensional fluid since it couples to the transverse momentum, which is conserved. As a result, the Green-Kubo expressions for various transport coefficients diverge in dimensions $d \leq 2$, and the hydrodynamic equations become nonlocal in time and space; for a review, see Ref. 17.

In classical systems in equilibrium, LTT effects, while qualitatively very important, are rather small quantitatively and become pronounced only at times so large that the correlation function is already very small overall. In non-equilibrium classical systems the effects are much more important.^{18,19} In equilibrium quantum systems the corresponding effects can also be much larger, especially in systems with quenched disorder, where the quantum LTTs are often referred to as “weak-localization effects”.^{17,20} Still, the correlation functions considered to date decay as functions of time, albeit more slowly than a separation-of-time-scales argument would suggest. In this paper we show that in a quantum system as simple as interacting electrons with no quenched disorder, i.e., the simplest model of a metal, there are correlations that actually *grow* with time, and in some cases also with distance. This surprising result is a consequence of generic soft, or slowly decaying, excitations in a Fermi liquid in conjunction with the incomplete screening of the Coulomb interaction at nonzero frequencies. It is a dramatic illustration of the fact that the impossibility of separating microscopic and macroscopic time scales, which is present in classical kinetics, holds *a fortiori* in quantum systems.

II. PHASE-SPACE CORRELATION FUNCTIONS

In quantum statistical mechanics it is useful to consider correlation functions that depend on one or more imaginary-time variables $\tau \in [0, 1/T]$, with T being the temperature, or on the corresponding imaginary Matsubara frequencies, $i\omega_n = 2i\pi T(n + 1/2)$ for fermions, and $i\Omega_n = 2i\pi Tn$ for bosons (n integer). Functions defined for imaginary Matsubara frequencies can be analytically continued to all complex frequencies, and the underlying real-time dependence can be obtained by an inverse Laplace transform. The observables in a fermion systems can be expressed in terms of expectation values of products of field operators $\hat{\psi}^\dagger(\mathbf{x}, \tau)$ and $\hat{\psi}(\mathbf{x}, \tau)$ that depend on the position \mathbf{x} in addition to τ . Spin is not essential for our purposes, and we suppress it for now. Let us consider binary products of $\hat{\psi}^\dagger$ and $\hat{\psi}$, and an imaginary-time Wigner operator $\hat{W}(\mathbf{X}, \mathbf{x}; \mathcal{T}, \tau) = \hat{\psi}^\dagger(\mathbf{X} + \mathbf{x}/2, \mathcal{T} + \tau/2) \hat{\psi}(\mathbf{X} - \mathbf{x}, \mathcal{T} - \tau/2)$. In a field-theoretic formulation, $\hat{\psi}^\dagger(\mathbf{x}, \tau)$ and $\hat{\psi}(\mathbf{x}, \tau)$ correspond one-to-one to fermionic (i.e., Grassmann-valued) fields $\bar{\psi}(\mathbf{x}, \tau)$ and $\psi(\mathbf{x}, \tau)$,²¹ in terms of which we define a Wigner field

$$W(\mathbf{X}, \mathbf{x}; \mathcal{T}, \tau) = \bar{\psi}(\mathbf{X} + \mathbf{x}/2, \mathcal{T} + \tau/2) \times \psi(\mathbf{X} - \mathbf{x}/2, \mathcal{T} - \tau/2) \quad (1)$$

in analogy to the operator \hat{W} . In common applications of real-time Wigner operators or fields, \mathbf{X} and \mathcal{T} correspond to the “average” or “macroscopic” (presumed to be slow) length and time scale, and \mathbf{x} and τ to the “relative” or “microscopic” (assumed to be fast) scales. The definition of the Wigner field reflects the assumption that it is possible and useful to separate these two scales.^{5,7} In terms of it, the fluctuating particle number density is given by $n(\mathbf{X}, \mathcal{T}) = W(\mathbf{X}, \mathcal{T}; \mathbf{x} = 0, \tau = 0)$, and the equilibrium single-particle Green function by $G(\mathbf{x}, \tau) = \langle W(\mathbf{X}, \mathcal{T}; \mathbf{x}, \tau) \rangle$, where $\langle \dots \rangle$ denotes an average taken with the action governing the fermion system. If the average is taken in a non-equilibrium state, $\langle W \rangle$ also depends on \mathbf{X} and \mathcal{T} . In a real-time formalism, with macroscopic time T and microscopic time t , $\langle W(\mathbf{X}, \mathbf{x}; T, t) \rangle = -i G^<(\mathbf{X}, \mathbf{x}; T, t)$ is the Green function $G^<$ defined in Ref. 5. Its Fourier transform with respect to the microscopic variables, $g^<(\mathbf{X}, T; \mathbf{p}, \omega)$, is often interpreted as the density of particles with momentum \mathbf{p} and energy ω at the space-time point (\mathbf{X}, T) .^{5,22} Switching back to imaginary time and frequency, this identifies

$$\begin{aligned} \rho(\mathbf{X}, i\omega_n) &= T \int_0^{1/T} d\mathcal{T} d\tau e^{i\omega_n \tau} W(\mathbf{X}, \mathcal{T}, \mathbf{x} = 0, \tau) \\ &= \sum_{\sigma} \bar{\psi}_{n,\sigma}(\mathbf{X}) \psi_{n,\sigma}(\mathbf{X}) \end{aligned} \quad (2)$$

as the density of particles with energy ω_n at point \mathbf{X} , i.e., a spatial energy distribution. Restoring spin, the spatial

Fourier transform of ρ reads

$$\begin{aligned} \rho(\mathbf{k}, i\omega_n) &= \int d\mathbf{X} e^{-i\mathbf{k} \cdot \mathbf{X}} \rho(\mathbf{X}, i\omega_n) \\ &= \sum_{\mathbf{p}, \sigma} \bar{\psi}_{n,\sigma}(\mathbf{p} + \mathbf{k}/2) \psi_{n,\sigma}(\mathbf{p} - \mathbf{k}/2), \end{aligned} \quad (3)$$

where $\bar{\psi}_n(\mathbf{p}) = \sqrt{T/V} \int d\mathbf{x} e^{-i\mathbf{p} \cdot \mathbf{x}} \bar{\psi}(\mathbf{x}, \tau)$ and $\psi_n(\mathbf{p}) = \sqrt{T/V} \int d\mathbf{x} e^{i\mathbf{p} \cdot \mathbf{x}} \psi(\mathbf{x}, \tau)$, with $\mathbf{p} \cdot \mathbf{x} = \mathbf{p} \cdot \mathbf{x} - \omega_n \tau$, $\int d\mathbf{x} = \int d\mathbf{x} \int_0^{1/T} d\tau$, and V the system volume. ρ depends on a macroscopic wave vector \mathbf{k} , but a microscopic frequency ω_n . This is in contrast to the number density n , which depends on two macroscopic variables. To verify the physical interpretation of ρ we note that its expectation value determines the density of states $N(\omega)$ via

$$N(\omega) = \frac{-1}{\pi} \frac{1}{V} \text{Im} \langle \rho(\mathbf{k} = 0, i\omega_n \rightarrow \omega + i0) \rangle \quad (4a)$$

The zeroth frequency moment gives the particle number N . With $\eta = 0^+$ the usual convergence factor²³ and $n_F(\omega)$ the fermion distribution function we have

$$N = T \sum_n e^{i\omega_n \eta} \langle \rho(\mathbf{k} = 0, i\omega_n) \rangle = V \int d\omega n_F(\omega) N(\omega), \quad (4b)$$

and the first frequency moment gives the energy E carried by the particles,²⁴

$$\begin{aligned} E &= T \sum_n e^{i\omega_n \eta} i\omega_n \langle \rho(\mathbf{k} = 0, i\omega_n) \rangle \\ &= V \int d\omega n_F(\omega) \omega N(\omega). \end{aligned} \quad (4c)$$

III. THE ORDER-PARAMETER SUSCEPTIBILITY OF A FERMI LIQUID

A. Definitions, and Results

Let us now consider the four-fermion correlation function $C_{\rho\rho}(\mathbf{X} - \mathbf{Y}; i\omega_n, i\omega_m) = \langle \delta\rho(\mathbf{X}, i\omega_n) \delta\rho(\mathbf{Y}, i\omega_m) \rangle$, with $\delta\rho = \rho - \langle \rho \rangle$. This is motivated by two considerations. First, $C_{\rho\rho}$ provides information about the correlations of energy levels in the Fermi system: It is the second moment of the energy density distribution. Second, the quantity $\nu(\mathbf{k}, i\omega_n) = \rho(\mathbf{k}, i\omega_n) - \rho(\mathbf{k}, -i\omega_n)$ can be interpreted, in a technically precise sense, as an order parameter (OP) for the Fermi liquid.² $C_{\nu\nu}(\mathbf{k}; i\omega_n, i\omega_m) = \langle \delta\nu(\mathbf{k}, i\omega_n) \delta\nu(-\mathbf{k}, i\omega_m) \rangle$ is thus the (longitudinal) OP susceptibility in an ordered phase. We will come back to this interpretation below. Writing $C_{\rho\rho}$ in imaginary-time space, and using time-translational invariance, one sees that it consists of two distinct contributions. One piece (which one would call “disconnected” in a diagrammatic representation) is proportional to δ_{nm} , and a second, “connected” one, is proportional to T .²⁵ We focus

on the connected piece by putting $\omega_m = -\omega_n$ and eliminate the trivial factor of temperature by defining

$$C(\mathbf{k}, i\omega_n) = \frac{1}{VT} \langle \delta\rho(\mathbf{k}, i\omega_n) \delta\rho(-\mathbf{k}, -i\omega_n) \rangle, \quad (5)$$

which has a well-defined zero-temperature limit.²⁶ Since C depends on a microscopic time scale, the separation-of-time-scales assumption would suggest that the analytic continuation $C(\mathbf{k}, i\omega_n \rightarrow z)$ is an analytic function of the complex frequency z at $z = 0$, corresponding to exponential decay in imaginary or real frequency space. From ordinary LTT physics one might expect that a coupling between the fast and slow degrees of freedom will lead instead to a nonanalytic function of the form z^α , which would lead to a LTT of the form $1/t^{\alpha+1}$. We find that neither of these expectations is correct in general: In a Fermi liquid with a Coulomb interaction in $d = 2$ the real-time dependence of the correlation function C is

$$C(\mathbf{k} \rightarrow 0, t) \propto \kappa^2 \ln(\kappa/|\mathbf{k}|) t^2 \quad (d = 2) \quad (6a)$$

where κ is the screening wave number. That is, C *increases* with time as t^2 ; i.e., the correlations get *stronger* with increasing time. This behavior is cut off by a nonzero wave number k or, equivalently, by a finite linear system size L ; it is valid for times $t \ll \sqrt{L}\kappa/v_F\kappa$ (and t much larger than the microscopic time scale, see Sec. IV below), with v_F the Fermi velocity. In $d = 3$ the behavior is a LTT with $\alpha = 0$,

$$C(\mathbf{k} \rightarrow 0, t) \propto 1/v_F^3 t \quad (d = 3), \quad (6b)$$

which is valid for $t \ll L/v_F$. For asymptotically large times C decays exponentially, with the rate of decay going to zero as the wave number approaches zero or the system size goes to infinity.

Also of interest are the spatial correlations. For $i\omega_n \rightarrow 0$, i.e., for particles close to the Fermi surface, the spatial correlations decay only algebraically,

$$C(\mathbf{x}, i\omega_n \rightarrow 0) \propto \begin{cases} \sqrt{\kappa}/v_F^3 \sqrt{r} & (d = 2) \\ \kappa/v_F^3 r^2 & (d = 3) \end{cases} \quad (7)$$

for distances $r = |\mathbf{x}| \gg 1/\kappa$.

These results hold for clean systems. In the presence of quenched disorder the effects are even stronger. The time dependence in $d = 2$ is the same as in the clean case and given by Eq. (6a), but in $d = 3$ the correlation function does not decay with time for $t \ll L^2/D$,

$$C(\mathbf{k} \rightarrow 0, t) \propto 1/D^2 |\mathbf{k}| \quad (d = 3), \quad (8)$$

where D is the diffusion coefficient that characterizes the diffusive electron dynamics. The spatial correlations for particles near the Fermi surface grow quadratically with distance and remain constant in $d = 2$ and $d = 3$, respectively,

$$C(\mathbf{x}, i\omega_n \rightarrow 0) \propto \begin{cases} (1/D^3) r^2 & (d = 2) \\ 1/D^3 & (d = 3). \end{cases} \quad (9)$$

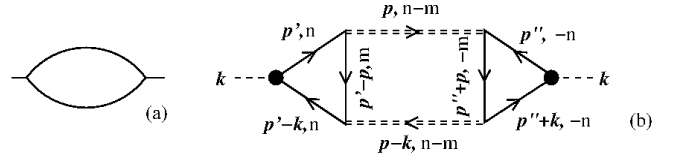


FIG. 1: Diagrammatic representation of the correlation function $C(\mathbf{k}, i\omega_n)$ for clean systems within (a) the effective field theory of Ref. 2, and (b) many-body perturbation theory. In (b), solid and double-dashed lines denote electronic Green functions and dynamically screened Coulomb potentials, respectively. Notice that no frequency is transferred at the external vertices (heavy dots); this reflects the fact that this is not a contribution to the usual density correlation function. The frequency conservation at the internal vertices is as usual.

These expressions are again valid for distances large compared to the microscopic length. Note that for particles at the Fermi surface ($i\omega_n = 0$) the spatial correlations at large distances in $d = 3$ get cut off only by the system size. In $d = 2$ they grow as the square of the distance for distances less than the localization length or the system size, whichever is smaller. See Sec. IV for a discussion of how to interpret this behavior.

B. Derivations

We now explain the origin and derivation of these surprising results. We first consider clean systems. The correlation function C , Eq. (5), can be calculated in various ways. In the framework of the effective field theory developed in Ref. 2 the leading contribution is given by the one-loop diagram shown in Fig. 1(a). The advantage of this framework is that the renormalization-group analysis of the effective theory guarantees that the result is the leading behavior; higher-loop diagrams will change the prefactor, but not the functional form of the result.³ Alternatively, the same result can be obtained from many-body perturbation theory²⁷ via the diagram shown in Fig. 1(b); however, there is no such guarantee within that formalism. A simplified analytical expression for either diagram, which has the correct scaling behavior, at $T \rightarrow 0$ is

$$C(\mathbf{k}, i\omega_n) \propto \int_k^\Lambda dp p^{d-1} \int_{\omega_n}^\infty d\omega \frac{1}{(\omega + v_F p)^4} (U(p, \omega))^2. \quad (10a)$$

Here Λ is an ultraviolet momentum cutoff, and $U(p, \omega)$ is the dynamically screened Coulomb interaction. For $\omega \gg v_F p$ in $d = 2, 3$ the latter has the structure

$$U(p, \omega) \approx \frac{\kappa^{d-1}}{p^{d-1} + \kappa^{d-1}(v_F p)^2/\omega^2}, \quad (10b)$$

where κ is the screening wavenumber. It shows the plasma frequency, $\omega_P \propto p^{3-d}$, and the incomplete screening at fixed nonzero frequency, $U(p \rightarrow 0, \omega) \propto 1/p^{d-1}$.

The factor of $1/(\omega + v_F p)^4$ represents the soft fermionic modes. In the effective field theory it results from the fact that the interacting part of the relevant propagator (the solid lines in Fig. 1(a)) scales as $1/(\omega + v_F p)^2$, that is, a simple ballistic propagator squared, see Eq. (S15c) in the Supplemental Material. Within many-body perturbation theory, each of the triangular fermion loops in Fig. 1(b) scales as $1/(\omega + v_F p)^2$. The strongly singular behavior discussed in Sec. III A results from a combination of these fermionic soft modes and the incomplete screening of the Coulomb interactions at nonzero frequencies. A short-range interaction still leads to singularities, but they are weaker than in the Coulomb case; the corresponding behavior is obtained by replacing $U(p, \omega)$ in Eq. (10a) by a constant. The limit on the time regime where Eq. (6a) is valid results from the most singular behavior of C in $d = 2$ being restricted to frequencies ω_n larger than the plasma frequency. Note that, in $d = 2$, the latter can be made arbitrarily small by going to small wave numbers (or to large system sizes at $\mathbf{k} = 0$).

For disordered systems, an appropriate effective field theory is the generalized nonlinear sigma model that has been studied extensively in the context of metal-insulator transitions.^{28–30} The relevant one-loop diagram is still given by Fig. 1(a), but the nature of the propagators is diffusive rather than ballistic, see Eq. (S13b) in the Supplemental Material. Within the framework of many-body perturbation theory the diagram shown in Fig. 1(b) needs to be dressed with diffusion poles in elaborate ways. The net result is that the factor $1/(\omega + v_F p)^4$ in Eq. (10a) gets replaced by a diffusion pole to the fourth power:

$$C(\mathbf{k}, i\omega_n) \propto \int_{\mathbf{k}}^{\Lambda} dp p^{d-1} \int_{\omega_n}^{\infty} d\omega \frac{1}{(\omega + Dp^2)^4} (U(p, \omega))^2, \quad (11a)$$

and the dynamically screened Coulomb potential gets modified to reflect the diffusive nature of the electron dynamics:

$$U(p, \omega) \approx \frac{\kappa^{d-1}}{p^{d-1} + \kappa^{d-1} D p^2 / (\omega + D p^2)}. \quad (11b)$$

Here D is the diffusion coefficient.

Performing the integrals in Eqs. (10) and (11) yields the results listed in Sec. III A.

IV. DISCUSSION

To discuss our results, we start with some remarks concerning the proper interpretation of Eq. (9). Consider a finite system of linear size L . The correlation function C in Eq. (9) then depends on two real-space positions, \mathbf{x} and \mathbf{y} . If L is increased by a factor of b , and \mathbf{x} and \mathbf{y} are scaled proportionally, so the distance $r = |\mathbf{x} - \mathbf{y}|$ also increases by a factor of b , then C increases by a factor of b^2 in $d = 2$. This is the meaning of the r^2 dependence in Eq. (9). On the other hand, if one increases r while keeping L fixed, then C decreases. For a discussion of this

point in a non-equilibrium context, see ch. 7.5 in Ref. 19. Analogous considerations apply in the time domain.

In the time domain, it is important to put the range of validity of Eqs. (6) in an appropriate context. The relevant microscopic time scale in a Fermi liquid is the inverse Fermi energy, which is on the order of 10^{-16} s in a good metal. For a macroscopic system with a linear size on the order of 1 cm, Eq. (6a) is valid for times at least four orders of magnitude larger than the microscopic scale, and Eq. (6b) is valid for times that are longer by yet another factor of 10^4 .

We suggest two ways to experimentally observe the effects discussed here: The first one is a direct measurement of the energy-density distribution, i.e., the spatial density of particles whose energy is in a certain interval. As discussed in conjunction with Eqs. (4) and (5), the correlation function C is the second moment of this distribution. We can think of no way to measure this distribution in a condensed-matter system, but it may be possible in a cold-atom system. The second one is in principle possible in a condensed-matter system. As can be seen from Eq. (4a), the density ρ defined in Eq. (2) determines the local density of states. The correlation function C thus contains information about the density-of-states fluctuations in the system. A two-tip tunneling experiment that measures the local density of states at points a fixed distance apart, repeated for different distances and covering the whole sample, would in principle be able to probe the long-range correlations we predict.

We finally add some remarks to put this remarkable behavior in context.

(1) As mentioned after Eq. (4c), the correlation function C can be interpreted as an OP susceptibility for the Fermi liquid. An interesting analogy in this context is the corresponding OP susceptibility in a classical Heisenberg ferromagnet. Due to a coupling between the longitudinal and transverse magnetization fluctuations the longitudinal magnetic susceptibility χ_L (i.e., the OP susceptibility) for $2 < d < 4$ diverges everywhere in the ordered phase as $1/k^{4-d}$.^{31,32} This results from a one-loop contribution to χ_L that is a wave-number convolution of two Goldstone modes, each of which scales as an inverse wave number squared. Diagrammatically this contribution has the same form as Fig. 1(a). To see the origin of the stronger effects discussed here, consider the spatial variation of χ_L as a function of the distance. Setting all wave-number components except for k_x equal to zero, we have

$$\chi_L(x \approx L) = \int_{1/L} d\mathbf{k}_x e^{i\mathbf{k}_x L} \chi_L(\mathbf{k}_x) \propto L^{3-d}. \quad (12)$$

That is, the correlations grow with the system size for $2 < d < 3$. The discussion at the beginning of the current section again applies. Our results for the Fermi-liquid OP susceptibility C are in direct analogy to this result if one makes the following adjustments: (i) For the time or frequency dependence, replace the only nonzero wave-number component k_x by the frequency and put $\mathbf{k} = 0$.

(ii) Realize that the relevant propagator in the quantum field theory² scales as a soft mode squared, see Eq. (10a) and Eq. (S15c) in the Supplemental Material. In the many-body calculation, this is apparent from the triangular fermion loops in Fig. 1(b), each of which scales as a ballistic propagator squared. (iii) Take into account the incomplete screening of the Coulomb interaction, which enhances the effect compared to the naive expectation that the quantum result should correspond to the classical one in an effective dimension $d_{\text{eff}} = d + 1$ (the relevant dynamical exponent is that of the fermionic soft modes, $z = 1$).

(2) The temporal and spatial dependences of the correlation function C are quite different: The underlying correlation is a function of two points in space, but four points in time; translational invariance implies that one and three of these, respectively, are independent. The time dependence of the function C results from having integrated over two of the three independent time arguments, which is justified by the physical interpretation of the function C . A related point is that we study the behavior of C for both frequency arguments approaching the Fermi surface, $\omega_n = -\omega_m \rightarrow 0$, rather than for large frequency differences. The spatial dependence of

C , on the other hand, has the same structure as in usual two-point correlation functions. An important result is that the spatial correlations become more and more long ranged as the Fermi surface is approached.

(3) In the classical-magnet analog the strong fluctuations eventually lead to an instability of the ordered phase at the ferromagnetic transition. In the present case, this suggests the possibility of a transition from a Fermi liquid to a non-Fermi liquid with a vanishing density of states at the Fermi surface.³³

(4) Studies of the distribution of the local density of states in disordered metals^{34,35} have calculated a different correlation function: viz., the disorder average of the *disconnected* piece of the correlation function $C_{\nu\nu}$ defined after Eq. (4c). The effects considered were thus entirely determined by disorder fluctuations and vanish in the clean limit. In contrast, the effects considered here are caused by the electron-electron interaction, and some of them are further enhanced by disorder.

We thank Thomas Vojta for discussions. This work was supported by the NSF under grant Nos. DMR-1401410 and DMR-1401449. Part of this work was performed at the Aspen Center for Physics and supported by the NSF under grants No. PHY-10-66293.

-
- ¹ D. Forster, *Hydrodynamic Fluctuations, Broken Symmetry, and Correlation Functions* (Benjamin, Reading, MA, 1975).
 - ² D. Belitz and T. R. Kirkpatrick, Phys. Rev. B **85**, 125126 (2012).
 - ³ See Supplemental Material for details.
 - ⁴ N. Bogoliubov, in *Studies in Statistical Mechanics*, edited by J. de Boer and G. Uhlenbeck (North-Holland, Amsterdam, 1962), vol. I.
 - ⁵ L. P. Kadanoff and G. Baym, *Quantum Statistical Mechanics* (W.A. Benjamin, New York, 1962).
 - ⁶ D. C. Langreth and J. W. Wilkins, Phys. Rev. B **6**, 3189 (1972).
 - ⁷ J. Schwinger, L. L. DeRaad, Jr., K. A. Milton, and W.-Y. Tsai, *Classical Electrodynamics* (Westview Press, 1998).
 - ⁸ R. L. Allen and D. W. Mills, *Signal Analysis* (Wiley-IEEE Press, Piscataway, NJ, 2004).
 - ⁹ B. J. Alder and T. E. Wainwright, Phys. Rev. Lett. **18**, 988 (1967).
 - ¹⁰ J. R. Dorfman and E. G. D. Cohen, Phys. Rev. Lett. **25**, 1257 (1970).
 - ¹¹ M. H. Ernst, E. H. Hauge, and J. M. J. van Leeuwen, Phys. Rev. Lett. **25**, 1254 (1970).
 - ¹² J. R. Dorfman and E. G. D. Cohen, Phys. Rev. Lett. **16**, 124 (1965).
 - ¹³ J. Weinstock, Phys. Rev. A **140**, 460 (1965).
 - ¹⁴ R. Peierls, *Surprises in Theoretical Physics* (Princeton University Press, 1979).
 - ¹⁵ S. Nagel, Rev. Mod. Phys. **64**, 321 (1992).
 - ¹⁶ J. R. Dorfman, T. R. Kirkpatrick, and J. V. Sengers, Ann. Rev. Phys. Chem. **45**, 213 (1994).
 - ¹⁷ D. Belitz, T. R. Kirkpatrick, and T. Vojta, Rev. Mod. Phys. **77**, 579 (2005).
 - ¹⁸ T. R. Kirkpatrick, E. G. D. Cohen, and J. R. Dorfman, Phys. Rev. A **26**, 995 (1982).
 - ¹⁹ J. M. Ortiz de Zárate and J. V. Sengers, *Hydrodynamic fluctuations in fluids and fluid mixtures* (Elsevier, Amsterdam, 2007).
 - ²⁰ P. A. Lee and T. V. Ramakrishnan, Rev. Mod. Phys. **57**, 287 (1985).
 - ²¹ J. W. Negele and H. Orland, *Quantum Many-Particle Systems* (Addison-Wesley, New York, 1988).
 - ²² G. D. Mahan, *Many-Particle Physics* (Kluwer, New York, 2000), 3rd ed., sec. 3.7.1.
 - ²³ A. L. Fetter and J. D. Walecka, *Quantum Theory of Many-Particle Systems* (McGraw-Hill, New York, 1971), secs. 23, 25.
 - ²⁴ More precisely, the right-hand side of Eq. (4c) equals $U + U_{\text{pot}} - \mu N$, where U and U_{pot} are the internal and potential energy, respectively, N is the particle number, and μ is the chemical potential²³.
 - ²⁵ The factor of T in the connected piece is a T^2 from the Fourier transforms of the fermion fields times a $1/T$ from a free imaginary-time integral. In a real-time formalism, the latter gets replaced by a free real-time integral which makes the correlation function proportional to an observation-time interval. C defined in Eq. (5) has a well-defined $T = 0$ limit given by the corresponding real-time function normalized by the observation time.
 - ²⁶ A related but different correlation function that shares some properties with the C defined here has been discussed in Ref. 36.
 - ²⁷ A. A. Abrikosov, L. P. Gorkov, and I. E. Dzyaloshinski, *Methods of Quantum Field Theory in Statistical Physics* (Dover, New York, 1963).
 - ²⁸ A. M. Finkelstein, Zh. Eksp. Teor. Fiz. **84**, 168 (1983),

- [Sov. Phys. JETP **57**, 97 (1983)].
- ²⁹ D. Belitz and T. R. Kirkpatrick, Phys. Rev. B **56**, 6513 (1997).
- ³⁰ D. Belitz and T. R. Kirkpatrick, Rev. Mod. Phys. **66**, 261 (1994).
- ³¹ V. G. Vaks, A. I. Larkin, and S. A. Pikin, Zh. Eksp. Teor. Fiz. **53**, 1089 (1967), [Sov. Phys. JETP **26**, 647 (1968)].
- ³² E. Brézin and D. J. Wallace, Phys. Rev. B **7**, 1967 (1973).
- ³³ T. R. Kirkpatrick and D. Belitz, Phys. Rev. Lett. **108**, 086404 (2012).
- ³⁴ I. V. Lerner, Phys. Lett. A **133**, 253 (1988).
- ³⁵ A. Andreev, B. D. Simons, and B. L. Altshuler, J. Math. Phys. **37**, 4968 (1996).
- ³⁶ T. R. Kirkpatrick and D. Belitz, EPL **102**, 17002 (2013).